ELSEVIER

Biochimica et Biophysica Acta 1421 (1999) 317–328

BIOCHIMICA ET BIOPHYSICA ACTA
BBA

www.elsevier.com/locate/bba

Fluid phase endocytosis and galactosyl receptor-mediated endocytosis employ different early endosomes

Marianne Synnes [b,1], Kristian Prydz [a,1], Torunn Løvdal [b], Andreas Brech [b], Trond Berg [b,*]

[a] *Department of Biochemistry, University of Oslo, Oslo, Norway*
[b] *Division of Molecular Cell Biology, Institute of Biology, University of Oslo, P.O. Box 1050, Blindern, 0316 Oslo, Norway*

Received 11 December 1998; received in revised form 4 August 1999; accepted 5 August 1999

Abstract

Endocytosis may originate both in coated pits and in uncoated regions of the plasma membrane. In hepatocytes it has been shown that fluid phase endocytosis (here defined as 'pinocytosis') is unaffected by treatments that arrest coated pit-mediated endocytosis, indicating that pinocytosis is primarily a clathrin-independent process. In this study we have tried to determine possible connections between pinocytosis and clathrin-dependent endocytosis in rat hepatocytes by means of subcellular fractionation, electron microscopy, and by assessing the influence of inhibitors of clathrin-dependent endocytosis on pinocytosis. As marker for clathrin-dependent endocytosis was used asialoorosomucoid (AOM) labelled with [^{125}I]tyramine cellobiose ([^{125}I]TC). [^{125}I]TC-labelled bovine serum albumin ([^{125}I]TC-BSA) was found to be a useful marker for pinocytosis. Its uptake in the cells is not saturable, and any remnants of [^{125}I]TC-BSA associated with the cell surface could be removed by incubating the cells with 0.3% pronase at 0°C for 60 min. The data obtained by electron microscopy and by subcellular fractionation suggested that early after initiation of uptake (<15 min) [^{125}I]TC-BSA and [^{125}I]TC-AOM were present in different endocytic vesicles. The two probes probably join prior to their entrance in the lysosomal compartment. The relation between endocytosis via coated pits and pinocytosis was also studied with techniques that induced a selective density shift either in the clathrin-dependent pathway (by AOM-HRP) or in the pinocytic pathway (by allowing uptake of AuBSA). Both treatments indicated that the two probes ([^{125}I]TC-AOM and [^{125}I]TC-BSA) were early after uptake, at least partly, in separate endocytic compartments. The different distribution of the fluid phase marker and the ligand (internalised via coated pits) was not due to a difference in the rate at which they enter a later compartment, since a lowering of the incubation temperature to 18°C, which should keep the probes in the early endosomes, did not affect their early density distribution. Incubation of cells in a hypertonic medium reduced uptake both of [^{125}I]TC-AOM and [^{125}I]TC-BSA; the uptake of [^{125}I]TC-AOM was, however, reduced much more than that of the fluid phase marker. This finding supports the notion that the two probes enter the cells via different routes.

Keywords: Hepatocyte; Endocytosis; Subcellular fractionation; Clathrin; Fluid phase

Abbreviations: ^{125}-TC-AOM, [^{125}I]tyramine-cellobiose-asialoorosomucoid; [^{125}I]TC-BSA, [^{125}I]tyramine-cellobiose-bovine serum albumin; β-AGA, *N*-acetyl-β-D-glucosaminidase

* Corresponding author. Fax: +47-22-85-46-05.

[1] Authors who contributed equally to this work.

0005-2736/99/$ – see front matter
PII: S0005-2736(99)00134-0

1. Introduction

Hepatic endocytosis plays an important role in controlling the level of macromolecules and particles in the blood. At least four types of cells participate in this process: the parenchymal cells (hepatocytes), the liver macrophages (Kupffer cells), the liver endothelial cells, and the stellate cells. It is generally accepted that endocytosis may take place both via a clathrin-dependent pathway and by clathrin-independent mechanisms [23,33]. Hansen et al. [18] demonstrated that clathrin-independent endocytosis in HEp-2 cells leads to the formation of small primary endosomes that fuse with the early endosomes that also receive input from clathrin-coated vesicles. Clathrin-independent endocytosis includes macropinocytosis [20,31,40] and maybe also potocytosis via caveolae [37].

Liver parenchymal cells express a number of receptors that mediate endocytosis of different ligands (e.g., epidermal growth factor [13,17], asialoglycoproteins [38,39], lipoproteins [19] and peptide hormones [1,2,30]). The exact mode of endocytosis is not known in all cases, although it has been generally assumed that hepatic receptor-mediated endocytosis takes place via coated pits. A paradoxical finding made by Weigel and coworkers is that fluid phase endocytosis in hepatocytes is nearly unaffected by treatments that effectively reduce uptake via coated pits: hypertonic medium as well as potassium depletion blocked receptor-mediated endocytosis of asialoorosomucoid but had only a modest effect on the fluid phase endocytosis of [^{14}C]sucrose and lucifer yellow [24–26]. These data indicate that the amount of fluid that out of necessity must be internalised via coated pits is negligible in comparison with that internalised via a clathrin-independent pathway. In other words, if the size of the primary endosomes formed by the clathrin-independent pathway is similar to that of the clathrin-coated vesicles, then a major proportion of the endocytosed plasma membrane must be internalised outside coated pits in the hepatocytes.

The purpose of the present study was to determine to what extent clathrin-dependent endocytosis and clathrin-independent endocytosis are separate pathways in rat hepatocytes and at what stage the two pathways eventually merge. To conduct such studies both pathways should preferably be allowed to operate in the absence of modulators, that in previous studies have been applied to block or stimulate one of the pathways in question. By subcellular fractionation in combination with density shift techniques, it was possible to separate early endocytic organelles containing a fluid phase marker from those with a marker taken up by endocytosis from coated pits. Moreover, the separate early endosomes could also be revealed by means of electron microscopy. The probes used for fluid phase endocytosis and clathrin-dependent endocytosis were bovine serum albumin (BSA) and asialorosomucoid (AOM), respectively. By labelling the probes with [^{125}I]TC it was possible to determine their net uptake since [^{125}I]TC is trapped in the degradative compartments [4]. [^{125}I]TC-AOM is taken up exclusively via coated pits [24] whereas [^{125}I]TC-BSA has been shown to be a reliable marker for the fluid phase of the forming endosome [36].

2. Materials and methods

2.1. Biochemicals

Collagenase was obtained from Sigma Chemical Co. (St. Louis, MO). Na^{125}I was from the Radiochemical Centre (Amersham, UK). All other chemicals were of analytical grade. As markers for clathrin-dependent endocytosis and fluid phase endocytosis were used asialoorosomucoid (AOM) and bovine serum albumin (BSA), respectively. The probes were labelled with [^{125}I]tyramine cellobiose ([^{125}I]TC) as described earlier [4].

2.2. Preparation of AOM-HRP

HRP (5 mg) was dissolved in 1 ml 0.3 M sodium bicarbonate buffer (pH 8.1), and 100 μl 0.04–0.08 M $NaIO_4$ was added. The solution was stirred carefully for 30 min at room temperature, 1 ml 0.16 M ethyleneglycol was then added, and careful stirring continued for 60 min. The solution was dialysed against 3×1 l sodium bicarbonate (0.01 M, pH 9.5) at 4°C. AOM (5 mg) in 1 ml sodium carbonate buffer was

added to 3 ml of the HRP-aldehyde solution and stirred carefully for 2–3 h at room temperature. $NaBH_4$ (5 mg) was added, and the solution was left for at least 3 h (or overnight) at 4°C. The resulting conjugate was dialysed against PBS at 4°C. Precipitates, if present, were removed by centrifugation.

2.3. Preparation of gold–AOM complexes

Colloidal gold (10 nm diameter) was made as described by Slot and Geuze [35]. Gold–AOM or gold–BSA complexes were prepared as follows. The pH of the solutions of gold and AOM (or BSA) was adjusted to 7.0 by means of NaOH [32] in order to optimise the adsorption of AOM to the gold particles [16]. The minimal concentration of AOM or BSA needed to stabilise the gold particles was found by adding 30 μl of AOM/BSA solution of increasing concentration to a series of tubes containing 200 μl gold solution. After 2 min 20 μl 10% NaCl was added, and the solution was shaken and left for 5 min. Electrolyte-induced aggregation of gold particles was seen as a change in colour from pink to blue. The procedure showed that 350 μg AOM or BSA per ml of 10-nm gold particle solution was an optimal AOM/BSA concentration. The gold–protein conjugates were separated from non-absorbed protein and clusters of gold by centrifugation (60 min at $25\,000 \times g$ in a Beckman Model J2-21 centrifuge at 4°C). The sediment was resuspended in PBS.

2.4. Cell preparation and incubation

Hepatocytes were prepared from 18h starved male Wistar rats (250–300 g) by collagenase perfusion [34]. The cells were incubated as suspensions (4-ml aliquots with shaking at 37°C, usually 50–75 mg wet wt./ml) in suspension buffer [34] fortified with pyruvate (20 mM) and Mg^{2+} (2 mM). To remove remnants of [^{125}I]TC-BSA possibly associated with the cell, the cells were routinely treated with 0.3% pronase at 0°C for 1 h. This treatment efficiently removed remnants of [^{125}I]TC-BSA, and the remaining radiolabelled probes were therefore associated with intracellular structures. No [^{125}I]TC-AOM would, on the other hand, remain bound to the plasma membrane since the cells were washed in Ca^{2+}-free solution [5].

2.5. Enzyme assays

β-Acetylglucosaminidase was determined according to Barrett [3].

2.6. Determinations of radioactivity

Radioactivities were measured in a Kontron gamma counter. Degradation of [^{125}I]TC-AOM and [^{125}I]TC-BSA was followed by measuring radioactivity soluble in 10% (w/v) trichloroacetic acid (acid-soluble radioactivity). Bovine serum albumin (0.5%) was added as a carrier.

2.7. Subcellular fractionation

Cell suspensions (in 0.25 M sucrose/10 mM Hepes/1 mM EDTA, pH 7.3) (referred to as homogenisation buffer)) were homogenised by 5 strokes in a Dounce homogeniser (tight-fitting pestle). The homogenates were fractionated by differential centrifugation or by isopycnic centrifugation in sucrose gradients. Differential centrifugation started by centrifuging a 5-ml sample of the homogenate at $2000 \times g$ for 2 min, the resulting nuclear fractions (N-fractions) were resuspended in 5 ml homogenisation buffer and centrifuged again at $2000 \times g$ for 2 min. From the postnuclear fractions were prepared sequentially M-fractions (at $6800 \times g$ for 4 min), L-fractions (at $22\,000 \times g$ for 9 min), P-fractions (at $48\,000 \times g$ for 60 min) and the final S-fractions. Differential centrifugation was carried out in a Sorvall RC-2B centrifuge using a SS-34 rotor and 13 ml centrifuge tubes. Homogenisation and centrifugations were carried out at 0–4°C. In isopycnic centrifugation experiments, 4-ml aliquots of a combined MLP-fraction or a P-fraction were initially layered on top of the gradients. The centrifuge tubes (38 ml) were centrifuged at $85\,000 \times g$ (25 000 rpm) in a Beckman SW 28 rotor at 4°C for 3 h. Following centrifugation the gradients were divided into 18×2 ml fractions by upward displacement using Maxidens as displacement fluid. The densities of the fractions were calculated from the refractive indices.

2.8. DAB-induced density shift of endosomes

The DAB-induced density modification [8,9] was based on the endocytic uptake of HRP-AOM followed by a cytochemical reaction on isolated subcellular fractions (mostly the postnuclear fraction). Hepatocytes (2 million cells/ml) were incubated with AOM-HRP (500 nM) at 37°C for the chosen time interval. Cells were washed in ice-cold 10% sucrose in 5-ml portions. Postnuclear fractions (5 ml) were subsequently prepared and incubated in the presence of DAB (3.2 ml) at room temperature in the dark for 15 min. Aliquots of the postnuclear fractions were then incubated in the presence and absence of H_2O_2 (36.8 μl 6% H_2O_2 added to 3.5 ml of postnuclear fraction) and the incubation was continued for another 30 min in the dark. The fractions were finally layered on top of linear sucrose gradients and centrifuged at $85\,000 \times g$ for 4 h.

2.9. Density shift induced by means of gold–BSA complex

Endosomal density shifts were also attempted at using AOM or BSA in complex with colloidal gold. The gold–AOM complexes were found to be unsuitable to induce a selective density shift of endosomes formed from coated pits, presumably because the complex also bound nonselectively to the plasma membrane. To induce endosomal density shift by means of gold–BSA, the cells were incubated at 37°C in presence of 100 nM BSA in complex with 10-nm gold particles (Au_{10}BSA).

2.10. Electron microscopy

Cells were incubated with AOM bound to 10-nm gold particles (Au_{10}AOM) or BSA bound to 5-nm gold particles (Au_5BSA). After 5 min incubation, the cells were washed in suspension buffer [34] containing 10 mM EGTA, and fixed in 2.0% glutaraldehyde in 0.1 M phosphate-buffered saline (PBS, pH 7.4) for 30 min at 4°C. The cells were then washed in PBS, postfixed for 60 min with 2% OsO_4 solution containing 1.5% potassium ferricyanide, and then stained with 1.5% uranyl acetate for 30 min. After dehydration in ethanol series, the cells were imbedded in Epon, sectioned and stained with 0.2% Pb-citrate. The sections were observed in a JEOL 100CX electron microscope at 80 kV.

3. Results

3.1. [^{125}I]TC-BSA as a fluid phase marker

Fig. 1 shows uptake of [^{125}I]TC-BSA in cells incubated at 4°C, or at 37°C in the presence or absence of 200 μM unlabelled BSA. Small amounts of [^{125}I]TC-BSA were found to be associated with the cells even at 0°C. This contaminating radioactivity, which amounted to less than 0.1% of total radioactivity added to the cells, was possibly associated with dead cells and could be completely removed by incubating the cells at 0°C with 0.3% pronase for 60 min. Fig. 1 shows results obtained in cells that had been treated with pronase following the incubation in presence of [^{125}I]TC-BSA. The amount of [^{125}I]TC-BSA taken up (about 0.1% of total radioactivity added per 10^6 cells per hour) corresponds to about 0.1 μl fluid per 10^6 cells per hour, and is in agreement with earlier data obtained with rat hepatocytes [24,26,36]. The results presented in Fig. 1

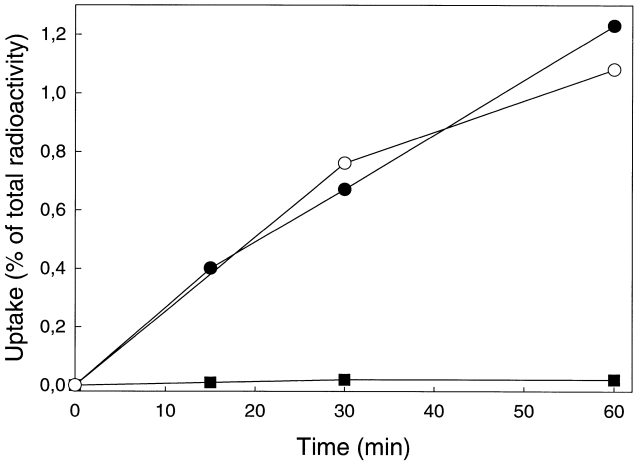

Fig. 1. The effect of a surplus of unlabelled BSA and reduced temperature on the uptake of [^{125}I]TC-BSA in rat hepatocytes. The cells (10^7 cells/ml) were incubated with 100 nM [^{125}I]TC-BSA at 4°C (■), or at 37°C with (○) or without (●) a surplus of unlabelled BSA (200 μM) added. Aliquots of cells were removed at the indicated time points and treated with 0.3% pronase for 1 h prior to measurement of cell-associated radioactivity. The uptake values are presented as percent of total radioactivity added to the cell suspension initially.

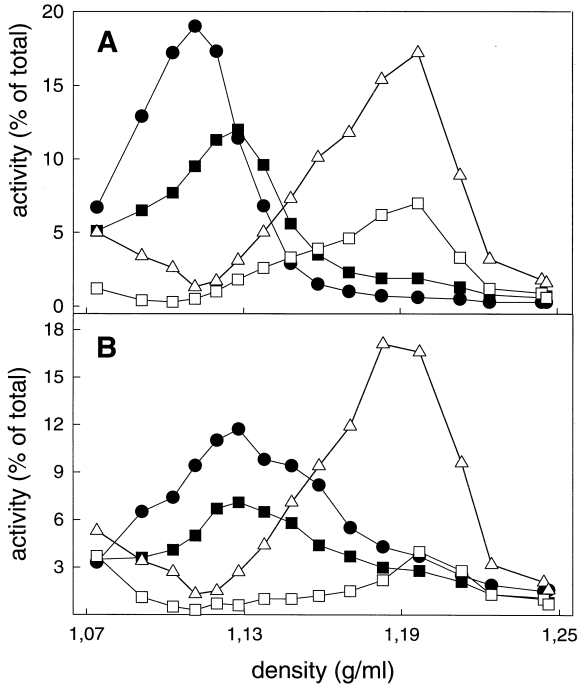

Fig. 2. Density distribution of endocytic organelles following isopycnic centrifugation of MLP-fractions from rat hepatocytes. [^{125}I]TC-AOM (A, 100 nM) and [^{125}I]TC-BSA (B, 100 nM) were added to suspensions of rat hepatocytes incubated at 37°C. Cells were removed from the incubator after 5 min (circles) or 60 min (squares), treated with 0.3% pronase for 1 h and homogenised. MLP-fractions were placed on top of linear sucrose gradients that were subsequently centrifuged for 3 h at 85 000×*g*. Acid-soluble (□) and acid-precipitable (■) radioactivities together with β-acetylglucosaminidase (△) were measured in the fractions derived from cells incubated for 60 min. Total radioactivity was measured in fractions from cells incubated for 5 min. The values are presented as percent of total recovered activity in the gradients.

shows that the uptake of [^{125}I]TC-BSA is not reduced in the presence of an excess of unlabelled BSA. Reducing the incubation temperature to 4°C reduced cell-associated radioactivity to low levels.

3.2. *Subcellular distribution of [^{125}I]TC-AOM and [^{125}I]TC-BSA following fractionation of cells by differential or sucrose density gradient centrifugation*

Following isopycnic centrifugation of MLP-fractions (Fig. 2), the [^{125}I]TC-AOM (Fig. 2A) was found in sequentially denser fractions: initially the ligand banded at 1.11 g/ml; it was subsequently found at 1.13 g/ml and after 15–30 min it started to appear as acid-soluble material banding at 1.19 g/ml. These data are in agreement with earlier observations [4,21]. [^{125}I]TC-BSA (Fig. 2B) seemed to enter an organelle that was denser than that accumulating [^{125}I]TC-AOM initially; the probe was eventually found in organelles coinciding with β-acetylglucosaminidase, presumably lysosomes (The labelled degradation products formed from the two probes are trapped in the degradative organelles and may therefore serve as markers for these compartments).

Since early endosomes containing [^{125}I]TC-BSA were denser than those containing [^{125}I]TC-AOM, we also studied the sedimentation properties of early endosomes containing the two types of probes by means of differential centrifugation, which separates organelles mainly on basis of differences in size. Previous studies have shown that [^{125}I]TC-AOM early after uptake is in endosomes that sediment in the P-fraction following differential centrifugation. Cells that had accumulated [^{125}I]TC-BSA for increasing time intervals were fractionated by classical differen-

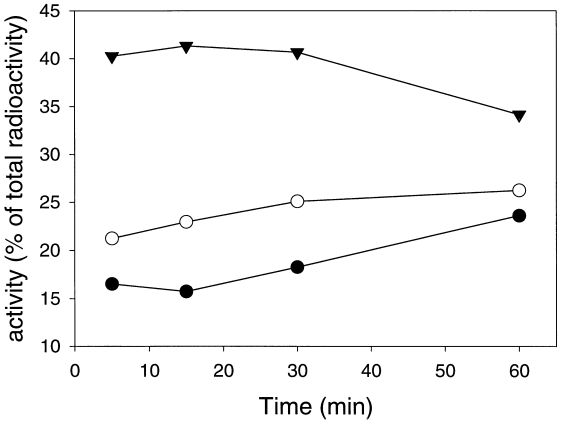

Fig. 3. Differential sedimentation of endocytic organelles of rat hepatocytes. [^{125}I]TC-BSA (100 nM) was added to suspensions of hepatocytes incubated at 37°C. Cells were removed from the incubator at the indicated time-points and treated with 0.3% pronase for 1 h. The cells were subsequently homogenised and fractionated by differential centrifugation into a nuclear, a mitochondrial, a light mitochondrial, a particulate, and a final supernatant fraction. Radioactivities were measured in the fractions. The results show the distribution of radioactivities in the mitochondrial (●), light mitochondrial (○) and particulate fractions (▼) at each time point, presented as percent of total radioactivity in the homogenate. The radioactivities in the combined nuclear and supernatant fractions amounted to between 16% and 22% of total radioactivity in the homogenate from which the fractions were prepared.

tial centrifugation [12] into N-, M-, L-, P-, and S-fractions. Fig. 3 indicates that the labelled probe was concentrated initially in the P- fractions and subsequently transferred to the denser mitochondrial fractions. Similar results have been obtained earlier for [^{125}I]TC-AOM [4].

Since both [^{125}I]TC-BSA and [^{125}I]TC-AOM enter early endosomes that sediment to a large extent in the P-fraction (Fig. 3), this fraction was subjected to isopycnic centrifugation to see whether the two probes coincided in the gradients, early (i.e., 10 min) after uptake in the cells. The results obtained are depicted in Fig. 4. [^{125}I]TC-AOM was, in agreement with earlier data, found in a band with peak activity at 1.11 g/ml. The bulk of the [^{125}I]TC-BSA was again found at higher density (1.15 g/ml). However, a minor peak of radioactivity was seen coinciding with the peak of [^{125}I]TC-AOM at 1.11 g/ml. This peak probably represents [^{125}I]TC-BSA that (out of necessity) is taken up via clathrin-coated pits.

3.3. Subcellular distribution of [^{125}I]TC-BSA and [^{125}I]TC-AOM in cells incubated at 18°C

The results obtained by subcellular fractionation indicated that [^{125}I]TC-BSA and [^{125}I]TC-AOM may to some extent enter the cells via different routes. The different distribution could possibly be due to different kinetics of internalisation: the fluid phase marker could conceivably be transferred rapidly via an early endosome (common for [^{125}I]TC-AOM and [^{125}I]TC-BSA) to a later denser compartment. To delay the [^{125}I]TC-BSA in a putative earlier compartment, the cells were incubated at 18°C to retard the intracellular transport. MLP- fractions from the cells were further fractionated in sucrose gradients. The density distributions of [^{125}I]TC-BSA and [^{125}I]TC-AOM shown in Fig. 5 (obtained with cells incubated at 18°C for 10 min) indicate again that the two probes are in different organelles.

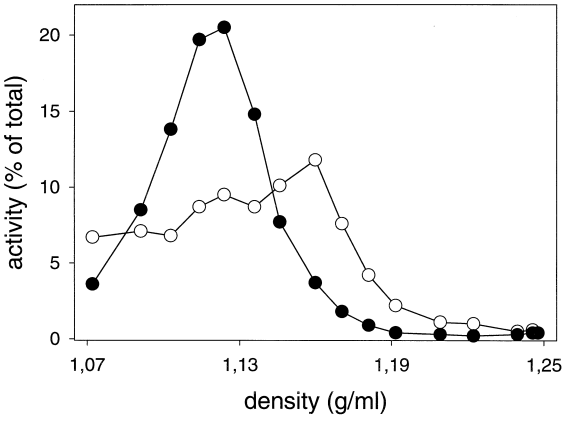

Fig. 4. Density distribution of endocytic organelles following isopycnic centrifugation of P-fractions from rat hepatocytes. [^{125}I]TC-BSA (○, 100 nM) or [^{125}I]TC-AOM (●, 100 nM) were added to suspensions of rat hepatocytes incubated at 37°C. Cells were removed from the incubator after 10 min), treated with 0.3% pronase for 1 h and homogenised. P-fractions were placed on top of linear sucrose gradients that were subsequently centrifuged for 3 h at 85 000×g. Radioactivities in the fractions are presented as percent of total recovered activity in the gradients.

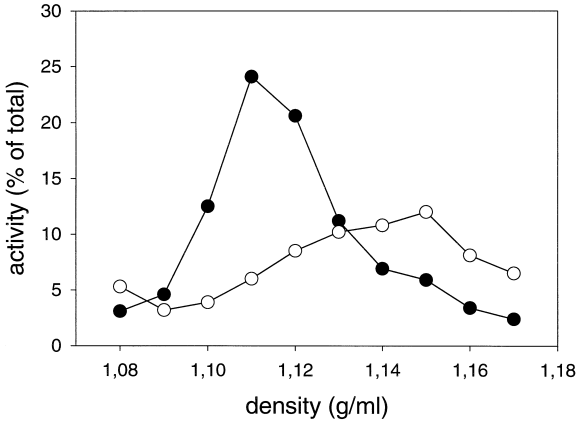

Fig. 5. Density distribution of endocytic organelles following isopycnic centrifugation of MPL-fractions from rat hepatocytes. Effects of reduced temperature. [^{125}I]TC-BSA (○, 100 nM) or [^{125}I]TC-AOM (●, 100 nM) were added to suspensions of rat hepatocytes incubated at 18°C. Cells were removed from the incubator after 10 min), treated with 0.3% pronase for 1 h and homogenised. MLP-fractions were placed on top of linear sucrose gradients that were subsequently centrifuged for 3 h at 85 000×g. Radioactivities in the fractions are presented as percent of total recovered activity in the gradients.

3.4. Density shift of endocytic organelles containing AOM-HRP by means of DAB/H_2O_2

To determine to what extent [^{125}I]TC-BSA and [^{125}I]TC-AOM were in separate endocytic compartments, the cells were preincubated with AOM-HRP to load the clathrin-dependent endocytic pathways, the cells were subsequently incubated with [^{125}I]TC-BSA or [^{125}I]TC-AOM for increasing time intervals, and density shifts were induced in endocytic vesicles

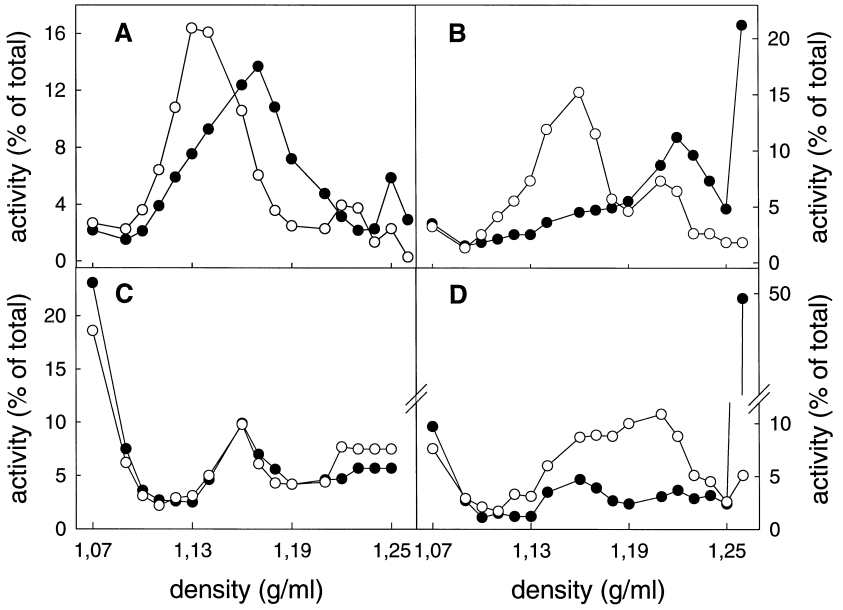

Fig. 6. DAB-induced density shift of [^{125}I]TC-AOM compared with that of [^{125}I]TC-BSA. [^{125}I]TC-AOM (A,B) or [^{125}I]TC-BSA (C,D) were added to rat hepatocytes that had been preincubated at 37°C with AOM-HRP (100 nM) for 30 min. The cells were treated with 0.3% pronase for 1 h and postnuclear fractions were prepared from the cells after 15 min (A,C) and 60 min (B,D). The postnuclear fractions were treated with DAB, with H_2O_2 (closed symbols) or without H_2O_2 (open symbols) as described in Section 2, and applied on top of sucrose density gradients. Radioactivities were assayed across the gradients.

containing AOM-HRP. It was found in preliminary experiments that the extent of density shift induced with DAB/H_2O_2 depended on the cell concentration with which AOM-HRP was incubated. A maximal density shift was obtained following incubation of cells (2×10^6 cells/ml) with 50 nM AOM-HRP. A further increase in AOM-HRP concentration did not increase the density shift induced by DAB/H_2O_2 (results not shown). Density shifts could only be observed if the AOM-HRP was inside endocytic vesicles. No density shift was observed when the AOM-HRP was added to the cell-free preparation of endosomes (not shown).

Fig. 6 shows that a density shift of endosomes containing [^{125}I]TC-AOM was seen, as expected, in cells that were incubated with AOM-HRP and [^{125}I]TC-AOM for 15 min (Fig. 6A); early endosomes containing [^{125}I]TC-BSA were not affected (Fig. 6C). At later time points (>15 min), density shifts were induced both in [^{125}I]TC-BSA- and [^{125}I]TC-AOM-containing endosomes (Fig. 6B,D). Fig. 6D shows that a small peak of radioactivity remains at 1.15 g/ml after treatment with H_2O_2/DAB even after 60 min. This peak evidently represents early endosomes that form continuously, since labelled [^{125}I]TC-BSA is present in the medium continuously.

3.5. *Effect of inducing density shift by means of gold–BSA complex*

We also tried to induce density shift by means of Au_{10}BSA. The results presented in Fig. 7 indicate clearly that the uptake of Au_{10}BSA does not affect the density distribution of early endosomes containing [^{125}I]TC-AOM, consistent with the notion that the two probes are internalised partly via separate pathways. At later time points, however, the density distribution of [^{125}I]TC-AOM was changed to higher densities by Au_{10}BSA (not shown). The two probes evidently meet in a late endosomal compartment, prior to their entrance into lysosomes.

3.6. *Effect of hypertonic medium on the uptake of [^{125}I]TC-BSA and [^{125}I]TC-AOM*

Certain treatments of cells have been used to differentiate between clathrin-dependent and clathrin-independent endocytosis: potassium depletion, hypertonic medium or acidification of cytosol have all

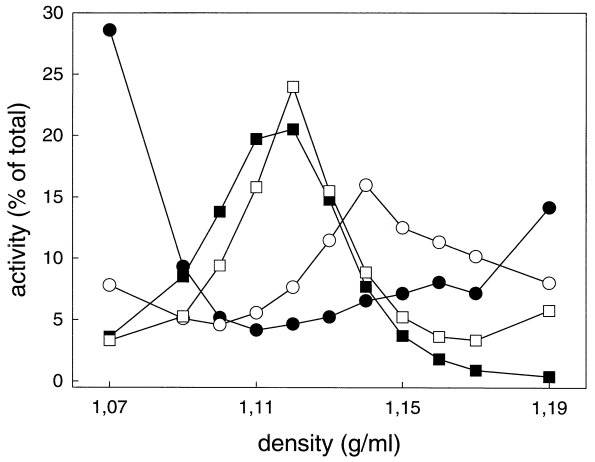

Fig. 7. Endocytic density shift induced by Au_{10}BSA. [^{125}I]TC-AOM (squares, 10 nM) or [^{125}I]TC-BSA (circles, 100 nM) were added to rat hepatocytes that had been preincubated at 37°C with (closed symbols) or without (open symbols) Au_{10}BSA (100 nM) for 30 min. Postnuclear fractions, prepared from cells (treated with 0.3% pronase for 1 h) after 5 min were applied on top of sucrose density gradients. Radioactivities were assayed across the gradients.

been shown to reduce clathrin-dependent endocytosis more than clathrin-independent endocytosis [33]. In the present study we found that all these treatments led to a reduced uptake of both probes. The uptake of [^{125}I]TC-AOM was, however, reduced significantly more than that of [^{125}I]TC-BSA. Fig. 8 shows the results of an experiment in which the cells were incubated with hypertonic medium (400 mosmol). The uptake of [^{125}I]TC-BSA was reduced to about 35% of controls whereas the corresponding value for [^{125}I]TC-AOM was about 10% (Fig. 8).

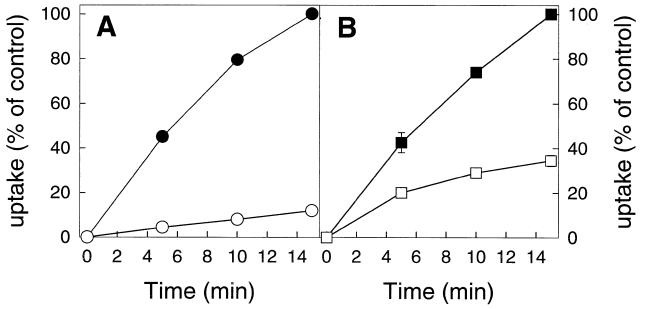

Fig. 8. Effect of hypertonic medium on the endocytosis of [^{125}I]TC-AOM and [^{125}I]TC-BSA. Hepatocytes were incubated at 37°C in incubation medium in the absence (closed symbols) or presence (open symbols) of 0.2 M sucrose. [^{125}I]TC-AOM (A, 100 nM) and [^{125}I]TC-BSA (B, 100 nM) were added to the cells and cell-associated radioactivities were determined in aliquots removed at the indicated time points. The cells were treated with 0.3% pronase at 0°C for 1 h prior to measurements of cell-associated radioactivity.

3.7. Electron microscopy

Fig. 9 shows Epon sections of hepatocytes that had internalised Au_{10}AOM and Au_5BSA for 5 min at 37°C. The electron micrographs indicate that Au_{10}AOM and Au_5BSA were internalised into separate endosomes early after uptake. Au_{10}AOM were found in clathrin-coated vesicles, whereas Au_5BSA could be found in larger vesicles in which no Au_{10}AOM could be observed (Fig. 9).

4. Discussion

Hepatocytes express numerous receptors that mediate endocytosis of macromolecules from blood [1,2,13,17,19,39]. In addition to uptake by receptor-mediated endocytosis the hepatocytes also internalise plasma constituents by fluid phase endocytosis [15,27]. Endocytosis involves internalisation of plasma membrane and may therefore contribute to the control of its composition of phospholipids and proteins. Of particular importance is the role of endocytosis in the control of the structure and function of the basolateral and the apical plasma membranes of hepatocytes [22].

Notwithstanding the physiological importance of hepatic endocytosis, relatively few studies have been done to characterise the modes of endocytosis in hepatocytes. It is generally accepted that endocytosis may take place both via clathrin-dependent and clathrin-independent pathways [23,33]. The present report shows, in agreement with earlier observations [24–26], that fluid phase endocytosis continues, albeit at a reduced rate, under conditions that block clathrin-dependent endocytosis of AOM. Such observations indicate that a major proportion of plasma membrane must be internalised via a clathrin-independent pathway, if one assumes that clathrin-dependent and clathrin-independent endocytosis lead to the formation of primary endosomes of comparable size. Extensive clathrin-independent endocytosis of plasma membrane in hepatocytes has been re-

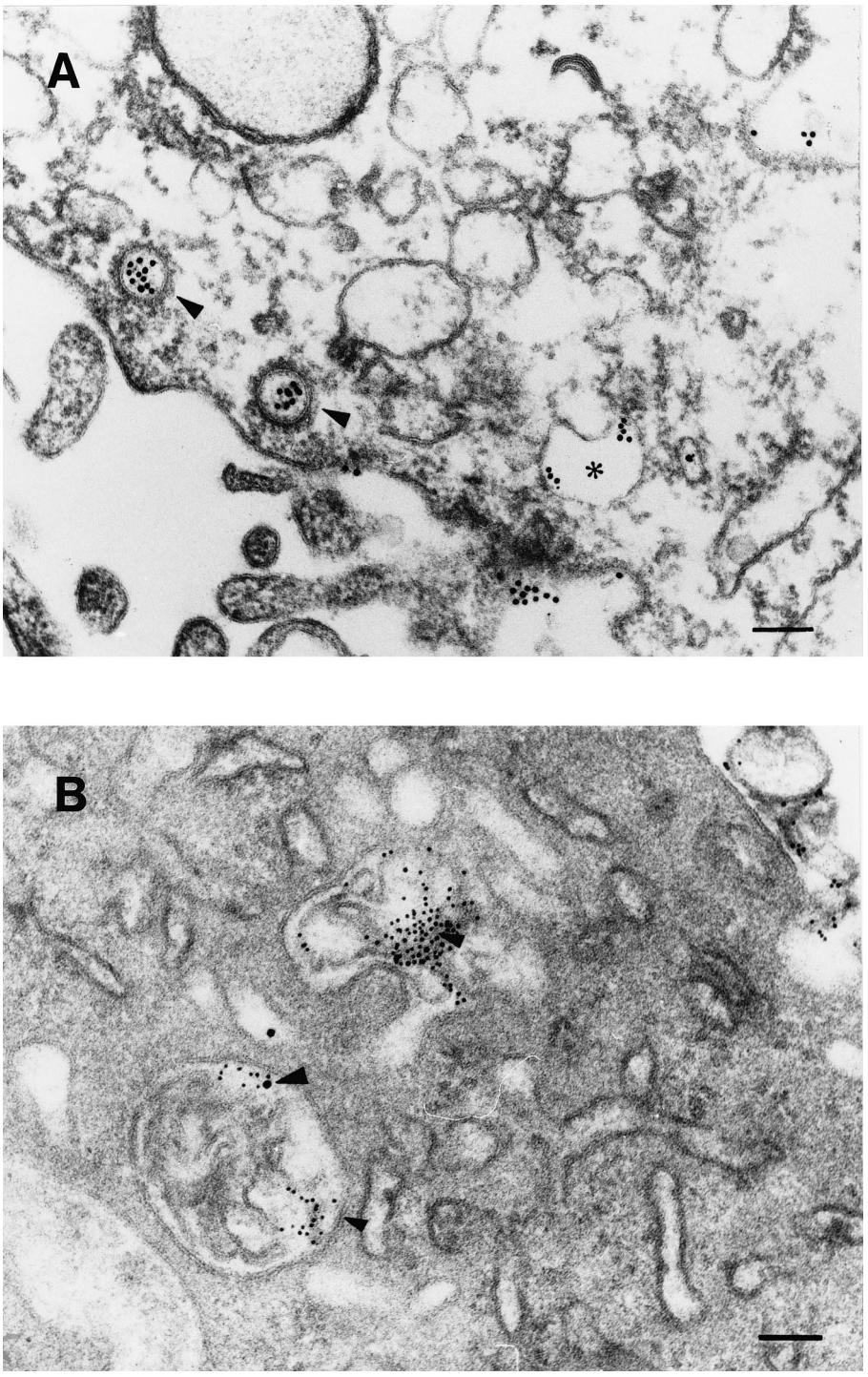

Fig. 9. Electron microscopy of hepatocytes that had internalised Au_{10}AOM and Au_5BSA were found in separate endosomes 5 min after internalisation. Hepatocytes were incubated for 5 min with Au_{10}AOM and Au_5BSA. The cells were washed in suspension buffer containing 10 mM EGTA prior to fixation at 4°C. A shows AuAOM in small, clathrin-coated vesicles, while B shows AuBSA in larger vesicles without clathrin coat. Bar = 100 nm.

cently demonstrated using ricin as a general marker of the plasma membrane [6].

Other studies have indicated that fluid phase endocytosis in hepatocytes may be nearly unaffected by the type of hypertonic treatment that was used in the present investigation. In our experiments the uptake of the fluid phase marker was reduced more than 50% by hypertonic medium. We do not know the reason for quantitatively different results. Part of the explanation may be the use of different types of fluid phase markers. We found, using labelled sucrose or raffinose, that hypertonic medium was without effect on the uptake of these probes. These low-molecular-mass probes were, however, found to penetrate the plasma membrane of hepatocytes at low temperature (data not shown), and were for this reason found unsuitable as markers for fluid phase endocytosis in our hands. A proportion of the fluid phase markers must, out of necessity, be internalised via coated pits and our subcellular fractionation data indicate indeed that some [^{125}I]TC-BSA coincide with [^{125}I]TC-AOM in sucrose gradients.

It is therefore reasonable that hypertonic medium also affects uptake of the fluid phase markers.

Inhibition of clathrin-dependent endocytosis may lead to a compensatory increase in clathrin-independent endocytosis [10,11]; the endocytosis observed in presence of inhibitors may therefore to some extent be an experimental artefact. The present study was initiated to try to get a direct estimation of the proportions of clathrin-dependent and clathrin-independent endocytosis. To this end subcellular fractionation was used combined with density shift techniques that presumably should selectively affect the density of endocytic organelles containing either [^{125}I]TC-AOM or [^{125}I]TC-BSA. As a marker for fluid phase endocytosis we used BSA labelled with [^{125}I]TC. This probe was, in accordance with an earlier report [36], found to be a reliable fluid phase marker in rat hepatocytes. By labelling BSA with [^{125}I]TC, it was possible to assess the true net uptake of the probe and to label organelles involved in its degradation [29].

Differential centrifugation combined with subcellular fractionation in sucrose density gradients indicated that most of the fluid phase marker was internalised into an early endosome that was denser than the early endosomes containing [^{125}I]TC-AOM. By using P-fractions as starting material for fractionation in sucrose gradients, some of the marker was found to coincide with the peak of [^{125}I]TC-AOM whereas the main peak was at a higher density. These data are consonant with the notion that [^{125}I]TC-BSA is mainly internalised via a clathrin-independent pathway. The peak coinciding with [^{125}I]TC-AOM shows, however, that some [^{125}I]TC-BSA is internalised via the coated pits. Uptake of a proportion of fluid phase marker via coated pits is also compatible with the finding that hypertonic medium reduced uptake of [^{125}I]TC-BSA. By inducing density shift in the endosomal pathway followed by [^{125}I]TC-AOM (by HRP-AOM combined with DAB/H_2O_2), it was again seen that the bulk of [^{125}I]TC-BSA entered a separate route. By using Au_{10}BSA it was verified that the fluid phase marker could be separated from the [^{125}I]TC-AOM early after uptake. It could be argued that the fluid phase marker may enter a late endocytic compartment more rapidly than [^{125}I]TC-AOM (which binds to the receptor) and that the separation of the two probes is due to a difference in the rate at which they enter the later compartment and not to different routes of entrance. The finding that a lowering of the incubation temperature, which should keep the probes in early endosomes [14], did not affect the density distribution of the probes, support the notion that [^{125}I]TC-BSA and [^{125}I]TC-AOM are to a large extent internalised via separate routes.

At what stage do the two pathways meet? Although some [^{125}I]TC-BSA evidently enters the same early endosome as [^{125}I]TC-AOM (Fig. 4), their main entrance routes are probably separate. Experiments using density shift techniques showed, on the other hand, that the two probes were degraded in the same lysosomes. Moreover, these techniques also indicated that an encounter of [^{125}I]TC-BSA and [^{125}I]TC-AOM took place even in a prelysosomal compartment, by definition a 'late' endosome. The late endosomes as a rendezvous for different types of endosomes is reminiscent of results obtained with polarised cells: in MDCK-cells, early endosomes from the basolateral and the apical plasma membrane meet in the same late endosomes [7, 28].

Acknowledgements

The study was supported by The Norwegian Research Council, Novo Nordisk Foundation, The Norwegian Cancer Society and Anders Jahres Foundation.

References

[1] F. Authier, B. Desbuquois, Degradation of glucagon in isolated liver endosomes. ATP-dependence and partial characterization of degradation products, Biochem. J. 280 (1991) 211–218.
[2] F. Authier, M. Janicot, F. Lederer, B. Desbuquois, Fate of injected glucagon taken up by rat liver in vivo. Degradation of internalized ligand in the endosomal compartment, Biochem. J. 272 (1990) 703–712.
[3] A. Barrett, in: J. Dingle (Ed.), Lysosomes; A Laboratory Handbook, Elsevier, Amsterdam, 1972, pp. 46–135.
[4] T.O. Berg, E. Stromhaug, T. Lovdal, O. Seglen, T. Berg, Use of glycyl-L-phenylalanine 2-naphthylamide, a lysosome-disrupting cathepsin C substrate, to distinguish between lysosomes and prelysosomal endocytic vacuoles, Biochem. J. 300 (1994) 229–236.
[5] R. Blomhoff, H. Tolleshaug, T. Berg, Binding of calcium ions to the isolated asialo-glycoprotein receptor. Implications for receptor function in suspended hepatocytes, J. Biol. Chem. 257 (1982) 7456–7459.
[6] A. Brech, R. Kjeken, M. Synnes, T. Berg, N. Roos, K. Prydz, Endocytosed ricin and asialoorosomucoid follow different intracellular pathways in hepatocytes, Biochim. Biophys. Acta 1373 (1998) 195–208.
[7] M.S. Bretscher, Circulating integrins: $\alpha_5\beta_1$, $\alpha_6\beta_4$ and Mac-1, but not $\alpha_3\beta_1$, $\alpha_4\beta_1$ or LFA-1, EMBO J. 11 (1992) 405–410.
[8] P.J. Courtoy, Analytical subcellular fractionation of endosomal compartments in rat hepatocytes, Subcell. Biochem. 19 (1993) 29–68. (review)
[9] P.J. Courtoy, J. Quintart, P. Baudhuin, Shift of equilibrium density induced by 3,3′-diaminobenzidine cytochemistry: a new procedure for the analysis and purification of peroxidase-containing organelles, J. Cell Biol. 98 (1984) 870–876.
[10] H. Damke, T. Baba, A. Van der Bliek, S.L. Schmid, Clathrin-independent pinocytosis is induced in cells overexpressing a temperature-sensitive mutant of dynamin, J. Cell Biol. 131 (1995) 69–80.
[11] H. Damke, T. Baba, D.E. Warnock, S.L. Schmid, Induction of mutant dynamin specifically blocks endocytic coated vesicle formation, J. Cell Biol. 127 (1994) 915–934.
[12] C. de Duve, B.C. Pressman, R. Gianetto, R. Wattiaux, F. Appelmans, Tissue fractionation studies. 6. Intracellular distribution patterns of enzymes in rat liver tissue, Biochem. J. 60 (1955) 604–617.
[13] W.A. Dunn, A.L. Hubbard, Receptor-mediated endocytosis of epidermal growth factor by hepatocytes in the perfused rat liver: ligand and receptor dynamics, J. Cell Biol. 98 (1984) 2148–2159.
[14] W.A. Dunn, A.L. Hubbard, N.N. Aronson Jr., Low temperature selectively inhibits fusion between pinocytic vesicles and lysosomes during heterophagy of [^{125}I]asialofetuin by the perfused rat liver, J. Biol. Chem. 255 (1980) 5971–5978.
[15] I.G. England, L. Naess, R. Blomhoff, T. Berg, Uptake, intracellular transport and release of [^{125}I]poly(vinylpyrrolidone) and [^{14}C]-sucrose-asialofetuin in rat liver parenchymal cells. Effects of ammonia on the intracellular transport, Biochem. Pharmacol. 35 (1986) 201–208.
[16] W.D. Geoghegan, G.A. Ackerman, Adsorption of horseradish peroxidase, ovomucoid and anti-immunoglobulin to colloidal gold for the indirect detection of concanavalin A, wheat germ agglutinin and goat anti-human immunoglobulin G on cell surfaces at the electron microscopic level: a new method, theory and application, J. Histochem. Cytochem. 25 (1977) 1187–1200.
[17] I.P. Gladhaug, T. Christoffersen, Kinetics of epidermal growth factor binding and processing in isolated intact rat hepatocytes. Dynamic externalization of receptors during ligand internalization, Eur. J. Biochem. 164 (1987) 267–275.
[18] S.H. Hansen, K. Sandvig, B. Van Deurs, The preendosomal compartment comprises distinct coated and noncoated endocytic vesicle populations, J. Cell Biol. 113 (1991) 731–741.
[19] R.J. Havel, R.L. Hamilton, Hepatocytic lipoprotein receptors and intracellular lipoprotein catabolism, Hepatology 8 (1988) 1689–1704.
[20] L.J. Hewlett, A.R. Prescott, C. Watts, The coated pit and macropinocytic pathways serve distinct endosome populations, J. Cell Biol. 124 (1994) 689–703.
[21] I. Holen, P.E. Stromhaug, P.B. Gordon, M. Fengsrud, T.O. Berg, P.O. Seglen, Inhibition of autophagy and multiple steps in asialoglycoprotein endocytosis by inhibitors of tyrosine protein kinases (tyrphostins), J. Biol. Chem. 270 (1995) 12823–12831.
[22] A.L. Hubbard, Targeting of membrane and secretory proteins to the apical domain in epithelial cells, Semin. Cell Biol. 2 (1991) 365–374.
[23] C. Lamaze, S.L. Schmid, The emergence of clathrin-independent pinocytic pathways, Curr. Opin. Cell Biol. 7 (1995) 573–580.
[24] J.A. Oka, M.D. Christensen, P.H. Weigel, Hyperosmolarity inhibits galactosyl receptor-mediated but not fluid phase endocytosis in isolated rat hepatocytes, J. Biol. Chem. 264 (1989) 12016–12024.
[25] J.A. Oka, P.H. Weigel, Effects of hyperosmolarity on ligand processing and receptor recycling in the hepatic galactosyl receptor system, J. Cell. Biochem. 36 (1988) 169–183.
[26] J.A. Oka, P.H. Weigel, The pathways for fluid phase and receptor-mediated endocytosis in rat hepatocytes are different but thermodynamically equivalent, Biochem Biophys. Res. Commun. 159 (1989) 488–494.

[27] L. Ose, T. Ose, R. Reinertsen, T. Berg, Fluid endocytosis in isolated rat parenchymal and non-parenchymal liver cells, Exp. Cell Res. 126 (1980) 109–119.
[28] R.G. Parton, K. Prydz, M. Bomsel, K. Simons, G. Griffiths, Meeting of the apical and basolateral endocytic pathways of the Madin-Darby canine kidney cell in late endosomes, J. Cell Biol. 109 (1989) 3259–3272.
[29] R.C. Pittman, T.E. Carew, C.K. Glass, S.R. Green, C.A. Taylor Jr., A.D. Attie, A radioiodinated, intracellularly trapped ligand for determining the sites of plasma protein degradation in vivo, Biochem. J. 212 (1983) 791–800.
[30] B.I. Posner, B.A. Patel, M.N. Khan, J.J. Bergeron, Effect of chloroquine on the internalization of [^{125}I]insulin into subcellular fractions of rat liver. Evidence for an effect of chloroquine on Golgi elements, J. Biol. Chem. 257 (1982) 5789–5799.
[31] E.L. Racoosin, J.A. Swanson, M-CSF-induced macropinocytosis increases solute endocytosis but not receptor-mediated endocytosis in mouse macrophages, J. Cell Sci. 102 (1992) 867–880.
[32] J. Roth, Application of lectin–gold complexes for electron microscopic localization of glycoconjugates on thin sections, J. Histochem. Cytochem. 31 (1983) 987–999.
[33] K. Sandvig, B. Van Deurs, Endocytosis without clathrin, Trends Cell Biol. 4 (1994) 275–277.
[34] P.O. Seglen, Preparation of isolated rat liver cells, Methods Cell Biol. 13 (1976) 29–83. (review)
[35] J.W. Slot, H.J. Geuze, A new method of preparing gold probes for multiple-labeling cytochemistry, Eur. J. Cell Biol. 38 (1985) 87–93.
[36] P.E. Stromhaug, T.O. Berg, T. Gjoen, P.O. Seglen, Differences between fluid-phase endocytosis (pinocytosis) and receptor-mediated endocytosis in isolated rat hepatocytes, Eur. J. Cell Biol. 73 (1997) 28–39.
[37] B. Van Deurs, P.K. Holm, K. Sandvig, S.H. Hansen, Are caveolae involved in clathrin-independent endocytosis, Trends Cell Biol. 3 (1993) 249–251.
[38] D.A. Wall, G. Wilson, A.L. Hubbard, The galactose-specific recognition system of mammalian liver: the route of ligand internalization in rat hepatocytes, Cell 21 (1980) 79–93.
[39] P.H. Weigel, Endocytosis and function of the hepatic asialoglycoprotein receptor, Subcell. Biochem. 19 (1993) 125–161. (review)
[40] M.A. West, M.S. Bretscher, C.A. Watts, Distinct endocytotic pathways in epidermal growth factor-stimulated human carcinoma A431 cells, J. Cell Biol. 109 (1989) 2731–2739.